THE PHYSICAL CONDITIONS IN THE PDR OF W49N

C. Vastel[1], M. Spaans[2], C. Ceccarelli[3], A. Tielens[2], and E. Caux[1]

[1]CESR CNRS-UPS, BP 4346, F-31028 - Toulouse cedex 04, France
[2]Kapteyn Astronomical Institute, PO Box 800, 9700 AV Groningen, The Netherlands
[3]Observatoire de Bordeaux, 2 rue de l'observatoire, BP 89, 33270 Floirac, France

Abstract

High resolution observations of the [CII] at 158 μm and [OI] 63, 145 μm with ISO-LWS are presented towards the ultracompact HII region W49N. Combined with other observational diagnostics from the literature (CO, far-infrared), theoretical models are constructed to constrain the physical conditions in the W49N photodissociation region. We compared this PDR with others galactic and extragalactic PDRs and found that the observed photo-electric heating efficiency is quite small (1-4 $\times 10^{-4}$). We then proceeded with a detailed model in order to determine the intensity of the cooling lines emitted by the PDR and compared them with observations. The major characteristics of the PDR in W49N is then an incident radiation field of $G_0 \approx 3 \times 10^5$ Habings and a density $n_{\rm H} \approx 10^4$ cm^{-3}.

Key words: ISM: abundances – ISM: molecules – ISM: atoms – HII regions – ISM: individual: W49N

1. Introduction

The W49N region is one of the most luminous regions of active star formation in the Galaxy. Located at $\sim$ 11.4 kpc (Gwinn et al. 1992), at about the same distance from the Galactic Center as the Sun, W49N generates a total bolometric luminosity of 6.8×10^6 L$_\odot$ (Buckley and Ward-Thompson 1996). Because of extremely high extinction at visible wavelength, this region can only by studied at radio and infrared wavelength. Welch et al. (1987) identified in its core at least ten distinct Ultra Compact HII regions, each powered by at least one O-type star, arranged in a partial 2-parsec ring.

In this paper, we report observations of several far-infrared and millimeter emission lines and use the fluxes from these lines to examine the physical properties of the emitting region. The FIR lines of [OI] (63 and 145 μm), [CII] (158 μm) observed with the LWS Fabry-Pérot on board ISO, and the rotational lines of CO observed with the SEST telescope provide important diagnostic tools for investigation of the physical conditions in Photo-Dissociation Regions (PDR; Tielens & Hollenbach 1985, hereinafter TH85). These regions of the interstellar medium are chemically affected by the strong FUV radiation emitted by nearby stars, which dissociates molecules and ionizes atoms. Because of luminosity considerations, the PDR emission in W49N is likely associated with the newly formed massive stars which are also responsible for ionizing the HII regions.

2. Observations

Figure 1 presents the observed [OI] 63 μm, 145 μm and 158 μm line profiles observed in the high spectral resolution mode of the LWS-ISO instrument. Notice that the 63 μm line presents a strong absorption feature, that affects the emission component of the HII region around 8 km/s. Vastel et al. (2000) separated this emission component from the absorption components due to cold molecular clouds in the velocity range [35 km s^{-1},70 km s^{-1}] along the line of sight. The line fluxes emitted by the central HII region are listed in table 1.

Table 1. Measured line fluxes from Fabry-Pérot spectra.

Line (μm)	Transition	Flux (10^{-10} erg s^{-1} cm^{-2})
[OI] 63.184	$^3P_1 \rightarrow {}^3P_2$	3.7 $\pm$ 0.2
[OI] 145.525	$^3P_2 \rightarrow {}^3P_3$	0.54 $\pm$ 0.06
[CII] 157.741	$^2P_{3/2} \rightarrow {}^2P_{1/2}$	1.27 $\pm$ 0.09

3. Characterisation of the PDR

The goal of this study is to determine the physical conditions in the PDR of the compact HII region W49N using the observed cooling lines as diagnostic.

3.1. Source geometry

The determination of the extent of the emitting infrared source is of prime importance in order to compute accurately the intrinsic line intensities. Harvey, Campbell and Hoffman (1977) mapped W49N at 53 μm with a 25$''$ (FWHM) beam and show that the source size is around 50$''$. Nevertheless we will considere it as a lower limit with an upper limit equal to the 80$''$ beam of the instrument.

Proc. Symposium *'The Promise of the Herschel Space Observatory'* 12–15 December 2000, Toledo, Spain
ESA SP-460, July 2001, eds. G.L. Pilbratt, J. Cernicharo, A.M. Heras, T. Prusti, & R. Harris

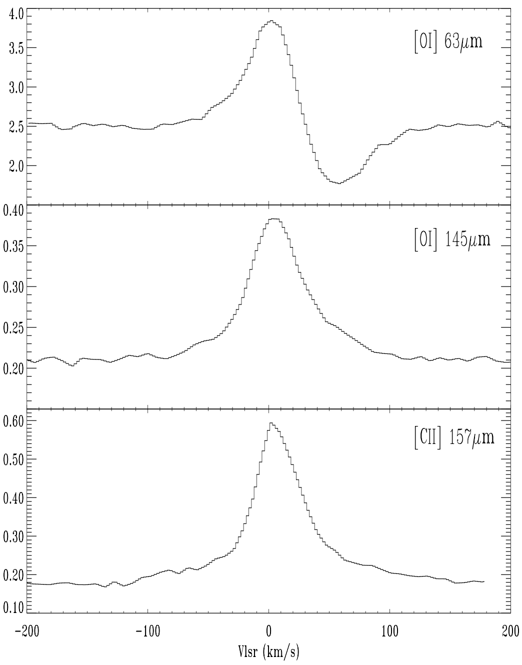

Figure 1. Comparison between the three observed lines at 63, 145 and 158 μm. Units are 10^{-8} erg s^{-1} cm^{-2} μm^{-1} and the emission line component is centered on the V_{LSR} of 8 km s^{-1} characteristic of the HII region.

3.2. PDR average parameters

In this paragraph we discuss how the [CII], [OI] and CO line emission and line-to-continuum ratio can constrain the physical conditions in the PDR, i.e. the average density and the intensity of the incident FUV radiation field. A method of parameterizing the FUV field incident on a cloud is through G_0. The observed integrated infrared intensity toward W49N of 33.5 erg s^{-1} cm^{-2} sr^{-1} (in a 50″ beam), implies that $G_0 = 3 \times 10^5$, assuming that the FUV is primarily responsible for heating the dust.

To derive the line intensities per unit solid angle we assumed an emitting region between 50″ and 80″ and a dust emitting region of 50″ as discussed in the previous paragraphs.

Using the value of G_0 of 3×10^5 computed with the observed integrated infrared intensity, we can estimate the density using the predictions of the Wolfire et al. (1990; hereinafter WTH90) PDR model. They presented especially useful contour plots of the fine-structure emission and line ratios predicted as a function of G_0 and n. The derived density is then 10^4 using the [CII] 158 μm/[OI] 63 μm ratio. Thus the G_0/n_H ratio is 30. Since [OI] 63 and 145 μm, [CII] 158 μm are expected to be the dominant cooling lines in PDRs with $G_0/n > 10^{-3}$ cm^3 (WHT90), the gas is heated by the grain photoelectric mechanism and the ratio between the total line intensity (obtained summing up the [OI] and [CII] line intensities) and the FIR continuum intensity gives the grain photoelectric heating efficiency ϵ, notably (1.4-3.6) $\times 10^{-4}$ in W49N. This is a relatively low value when compared with that of other studied PDRs, where $\epsilon \sim 3 \times 10^{-3}$ (see Tab. 3 and the discussion in Sec.5) and has to imply a high $G_0/n_{\rm H}$ which produces a strong decrease in ϵ because of the high positive grain charge.

The conditions, derived by WTH90 model, seem to indicate a PDR illuminated by a strong FUV radiation field.

Table 2. Model parameters.

Parameter	Symbol	Value
hydrogen particle density	$n_{\rm H}$ (cm^{-3})	10^4
FUV intensity	G_0	3×10^5
turbulent Doppler width	b (km s^{-1})	3.5
Carbon abundance	[C]	1.4×10^{-4}
Oxygen abundance	[O]	3.2×10^{-4}
PAH abundance	[PAH]	4×10^{-7}

4. PDR modeling

In the following section, we present the results of a detailed PDR model and determine the average density $n_{\rm H}$, the incident FUV flux G_0, and the chemical abundances as a function of the depth in the cloud. This model will constrain more accurately the physical conditions in the photodissociation region in W49N. Table 2 lists the set of adopted model parameters.

The results for the models with $G_0 = 3 \times 10^5$ and a density of 10^4 are compared to the observations in Table 3.

The lower limit of the observed [OI] 145 μm and [CII] 158 μm lines compares favorably with the model which is consistent with the assumption that the line emitting region tends to be 80″. Nevertheless, the comparaison between the upper limit of the observed [OI] 63 μm line and the model would imply a lower emitting region of 50″. Assuming this 50″ extend for the cooling lines, the optically thin [CII] 158 μm and [OI] 145 μm lines are somewhat low but still consistent within a factor of two with the observations. This discrepency is quite commeon in detailed model fits (cf Tielens and Hollenbach 1985) and may reflect geometry effects and/or differents dust extinction properties. For example a viewing angle of 60 % rather than a face-on would result in a factor 2 increase in the intensity of optically thin lines without affecting the intensity of optically thick lines (i.e. [OI] 63 μm and CO J $= 1 \rightarrow 0$) much. Alternatively, a 20 % change in the ratio of FUV dust absorption over visual extinction changes the column of warm gas (100 K at $A_v \sim 2$ mag) that emits these lines by a factor of 2.

Table 4. Comparison between W49N and similar sources. The line fluxes are in erg s^{-1} cm^2 sr^{-1} and ϵ is calculated as the ratio between the total cooling line intensity and the FIR (see text).

Sources	Distance (kpc)	I(63) 10^{-4}	I(145) 10^{-4}	I(158) 10^{-4}	I(CO(1-0)) 10^{-7}	I(FIR)	Log(G_0)	ϵ 10^{-4}	References
W49N	11.4	31-80	4.6-12	11-28	4.6	33.5	5.5	1.4-3.6	1
NGC2023	0.48	36	2.3	6.8	1.5	0.76	3.7	62	2
NGC7027	1.1	1200	45	130	3.1	60	5.7	23	3
M82	3300	120	5.3	17	2.7	50	4.7	33	4
Orion Bar	0.47	400	20	60	4	5	4.6	110	5
M17 SW	2.5	150	19	26	7	6.7	4.7	47	6
30 Doradus	49	0.92	0.69	5.9	0.24	0.78	3.7	9.6	7
M42	0.47	400-600	30-60	40-70	5.8	12	5	25	8
NGC7023	0.43	7.5	90	2.8	0.64	0.6	3.7	19	9
NGC2068	0.48	2.3	0.9	8.1	1.1	0.3	3.4	39	10
Galactic center 1	8.1	240	6.9	15	2.2-3.0	48	5.6	9.5	11
Galactic center 2	8.1	40	2.8	8.3	2.2-3.0	17	5.1	4	12

1) Vastel et al, 2001. 2) Steiman-Cameron 1997; Milman 1975. 3) Telesco and Harper 1977; Ellis and Werner 1984; Burton, Hollenbach and Tielens 1990. 4) Telesco and Harper 1977; Stacey et al. 1991; WTH90. 5) Tauber et al. 1994. 6) Meixner 1992. 7) Stacey 1991, Vastel 2000 (private communication). 8) Crawford et al. 1985; WTH90. 9) Chokshi 1988, Fuente et al. 2000. 10) Milman 1975. 11 and 12) offset of Δb = 0, Δl = 20$''$ for position 1, and Δb = 0, Δl = 80$''$ for position 2, from α_{2000} = 17h44m25.52s and δ_{2000} = 28^{o}58$'$1.7$''$ (WTH90).

Table 3. Comparison between the observations of W49N and the model results for the [OI] lines at 63 and 145 μm, [CII] at 158 μm, [SiII] at 35 μm, [CI] at 609 μm and CO at 2.6 mm. The lower (respectively upper) limit for the [OI] and [CII] lines corresponds to a 80$''$ (respectively 50$''$) source size. The intensities are in erg s^{-1} cm^{-2} sr^{-1}. Lines that are not observed are labeled as no.

	Obs.	Model G_0=3 × 10^5 $n_H = 10^4$
[OI](63 μm)	(3.1-8.0) 10^{-3}	8.0 10^{-3}
[OI](145 μm)	(4.6-12) 10^{-4}	5.0 10^{-4}
[CII](158 μm)	(1.1-2.8) 10^{-3}	1.4 10^{-3}
[SiII](35 μm)	no	1.9 10^{-4}
[CI](609 μm)	no	1.3 10^{-6}
CO(J = 1 → 0)	4.6 10^{-7}	5.8 10^{-7}
63/145	6.8	16.0
63/158	2.9	5.8
ϵ	(1.4-3.6) 10^{-4}	7.9 10^{-4}
CII/CO	(2.4-6.1) 10^3	2.4 10^3

5. Discussion

We now compare W49N to well known PDR templates associated with HII regions (30 Doradus, M17, M42), PDRs associated with reflection nebulae and planetary nebulae (NGC 2068, NGC 7023, NGC 2023, NGC7027), and PDRs associated with the nuclei of galaxies (M82). From Table 4, we find a similarity between the two galactic HII regions W49N and M17SW for the intensities of their cooling lines although the Far-infrared luminosity differ by a factor 5. W49N appears to be one of the most luminous HII regions in the FIR with NGC7027, M82 and Galactic center 1.

The UV field illuminating clouds in W49N, NGC7027 and the two positions of the galactic center is high (G_0 ∼ $10^{5.1}$-$10^{5.7}$) compared to other HII regions, resulting of a close association between sources of UV radiation and clouds and produced by an enhanced star formation rate. It is interesting to note that the average conditions in the starburst galaxy M82 are so similar to those in regions surrounding newly formed stars in our Galaxy.

It also appears that the compact HII region W49N is a peculiar source in terms of its heating efficiency which is a factor of ∼ 10 less than most others PDRs. Nevertheless, this value is comparable to the one obtained for the two positions in the direction of the galactic center and to the 30 Doradus nebula in the Large Magellanic Cloud. The low photoelectric heating efficiency (ϵ) determined for W49N has been explained in the previous sections by a high G_0/n of ∼ 30, estimated from a PDR modeling, which increase the positive grain charge and produces a strong decrease of ϵ. Indeed a higher charge implies a higher Coulomb barrier that has to be overcome. Thus a smaller fraction of the electrons moving onto the grain will escape, reducing the efficiency. It can be noticed that the sources presenting the lowest efficiencies ($\epsilon \leq 10^{-3}$) present a G_0/n greater than unity using the WTH90 model.

The W49N HII region is an extraordinary clear specimem of a very massive and very luminous photodissociation region. The extreme conditions emerging from this star-forming region require many other observations with a higher spectral resolution for example [SiII] and [CI] which is a tracer of the surface area of gas exposed to UV photons, a quantity that can be translated into a measure of the inhomogeneity of the medium.

6. Conclusion

The overall picture that arises from the observational data is that of a molecular cloud surrounding the HII region, illuminated by several O-type stars. The major characteristics of this source are:
1) a very low photoelectric heating efficiency ($\sim 10^{-4}$),
2) an intense FUV luminosity ($G_0 \sim 3 \times 10^5$).
These properties render W49N peculiar source with extreme physical conditions, but also one that can be accommodated naturally in the general PDR framework.

References

Buckley, H.D. and Ward-Thompson, D., 1996, MNRAS 281, 294

Burton, M.G., Hollenbach, D.J. & Tielens, A.G.G.M., 1990, ApJ 365, 620

Chokshi, A., Tielens, A.G.G.M., Werner, M.W., Castelaz, M.W., 1988, ApJ 334, 803

Crawford, M.K., Genzel, R., Townes, C.H. & Watson, D.M., 1985, ApJ 291, 755

Ellis, H.B. & Werner, M.W., 1984, AAS 16, 463

Fuente, A., Martin-Pintado, J., Rodriguez-Fernandez, N.J. et al., 2000, A&A 354, 1053

Gwinn, C.R., Moran, J.M. & Reid, M.J., 1992, ApJ 393, 149

Harvey, P.M., Campbell, M.F. & Hoffmann, W.F., 1977, ApJ 211, 786

Meixner, M., Haas, M.R., Tielens, A.G.G.M. et al, 1992, ApJ 390, 499

Milman, A.S., Knapp, G.R., Knapp, S.L., Wilson, W.J., 1975, AJ 80, 93

Spaans, M., 1996, A&A 307, 271

Spaans, M. & van Dishoeck, E., 1997, ApJ 323, 953

Stacey, G.J, Geis, N., Genzel, R., Lugten, J.B, et al., 1991, ApJ 373, 423

Steiman-Cameron, T.Y., Haas, M.R. & Tielens, A.G.G.M., 1997, ApJ 478, 261

Tauber, J.A., Tielens, A.G.G.M., Meixner, M. & Goldsmith, P.F., 1994, ApJ 422, 136

Telesco, C.M. & Harper, D.A., 1977, ApJ 211, 475

Tielens, A.G.G.M. & Hollenbach, D., 1985, ApJ 291, 747

Vastel, C., Caux, E., Ceccarelli, C., Castets, A. et al., 2000, A&A 357, 994

Vastel, C., Spaans, M., Ceccarelli, C., Tielens, A.G.G.M., Caux, E., 2001, *to be submitted*

Ward-Thompson, D. & Robson, E.I., 1990, MNRAS 244, 458

Welch, W.J., Dreher, J.W., Jackson, J.M., Terebey, S. and Vogel, S.N., 1987, Science 238, 1550

Wolfire, M.G., Tielens, A.G.G.M. & Hollenbach, D., 1990, ApJ 358, 116